AGU PUBLICATIONS

Geophysical Research Letters

RESEARCH LETTER
10.1002/2016GL070319

Key Points:
- A moored array measured bottom currents across Drake Passage with unprecedented resolution
- The mean barotropic Antarctic Circumpolar transport is 45.6 Sv ± 8.9 Sv
- The ACC transport of 173.3 Sv is 30% larger than the canonical value of 134 Sv

Supporting Information:
- Supporting Information S1
- Figure S1

Correspondence to:
K. A. Donohue,
kdonohue@uri.edu

Citation:
Donohue, K. A., K. L. Tracey, D. R. Watts, M. P. Chidichimo, and T. K. Chereskin (2016), Mean Antarctic Circumpolar Current transport measured in Drake Passage, *Geophys. Res. Lett.*, *43*, doi:10.1002/2016GL070319.

Received 7 JUL 2016
Accepted 27 OCT 2016
Accepted article online 1 NOV 2016

Mean Antarctic Circumpolar Current transport measured in Drake Passage

K. A. Donohue[1], K. L. Tracey[1], D. R. Watts[1], M. P. Chidichimo[2,3,4], and T. K. Chereskin[5]

[1]Graduate School of Oceanography, University of Rhode Island, Narragansett, Rhode Island, USA, [2]Consejo Nacional de Investigaciones Científicas y Técnicas (CONICET), Argentina, [3]Servicio de Hidrografía Naval, Buenos Aires, Argentina, [4]Universidad de Buenos Aires, Buenos Aires, Argentina, [5]Scripps Institution of Oceanography, University of California, San Diego, California, USA

Abstract The Antarctic Circumpolar Current is an important component of the global climate system connecting the major ocean basins as it flows eastward around Antarctica, yet due to the paucity of data, it remains unclear how much water is transported by the current. Between 2007 and 2011 flow through Drake Passage was continuously monitored with a line of moored instrumentation with unprecedented horizontal and temporal resolution. Annual mean near-bottom currents are remarkably stable from year to year. The mean depth-independent or barotropic transport, determined from the near-bottom current meter records, was 45.6 sverdrup (Sv) with an uncertainty of 8.9 Sv. Summing the mean barotropic transport with the mean baroclinic transport relative to zero at the seafloor of 127.7 Sv gives a total transport through Drake Passage of 173.3 Sv. This new measurement is 30% larger than the canonical value often used as the benchmark for global circulation and climate models.

1. Introduction

Considerable effort as part of the International Southern Ocean Studies (ISOS) program in the late 1970s and early 1980s led to the canonical Antarctic Circumpolar Current (ACC) mean transport estimate of 134 sverdrup (Sv) (1 Sv equals $10^6 m^3 s^{-1}$) [*Whitworth and Peterson*, 1985]. Up until then, estimates of geostrophic ACC transport from hydrographic sections varied widely, mainly due to uncertainty in the reference level applied to the strong deeply sheared ACC and a lack of information about the structure and strength of near-bottom currents. A pilot array of six near-bottom current meter moorings across Drake Passage [*Bryden and Pillsbury*, 1977] informed the final ISOS array design. These measurements revealed that a level of no motion at the seafloor would not be appropriate; mean along-passage deep velocities were on the order of 1–2 cm s^{-1} [*Bryden and Pillsbury*, 1977]. Ultimately, ACC mean and time-varying transport was determined from a suite of instrumentation including bottom-pressure gauges, dynamic-height and current-meter moorings, and hydrography using a combination of techniques [*Whitworth et al.*, 1982; *Whitworth*, 1983; *Whitworth and Peterson*, 1985]. *Cunningham et al.* [2003] conducted a careful reanalysis of the ISOS methodology and assumptions, updating the ISOS mean transport error to be 27 Sv. Few metrics in physical oceanography are as widely utilized as the mean ACC transport of 134 Sv. This number has been used to validate ocean and climate models, guide endpoints for ACC transport calculations in the open oceans away from ACC choke points, and set initial conditions for inverse models.

Accurate ACC transport estimates are required to assess how the Southern Ocean is responding to climate change. Conducting an ISOS-like campaign remains a costly endeavor. Contemporary approaches include repeat hydrographic [*Cunningham et al.*, 2003] and shipboard acoustic Doppler current profiler (SADCP) surveys [*Firing et al.*, 2011] and combining historical hydrography with Argo float displacements [*Colin de Verdière and Ollitrault*, 2016]. The advent of accurate satellite measurements of sea surface height and gravity permit transport estimation by combining observations from satellite altimeter with sparsely spaced current-meter moorings [*Koenig et al.*, 2014] and the synthesis of satellite altimeter and gravity missions [*Zlotnicki et al.*, 2007]. Each approach grapples with the transport calculation's demand for high spatial and temporal resolution particularly for the reference currents. Repeat hydrographic and SADCP surveys are subject to both temporal sampling issues and potential bias errors. *Meredith and Hughes* [2005] find that sampling on time scales of less than a week is required to determine an unaliased annual mean; more rapid sampling is required to resolve seasonal variations. Even at Drake Passage, the narrowest ACC choke point, an average through-passage flow

of 1 cm s^{-1} equates to about 30 Sv. Because the Subantarctic Front (SAF), the northernmost jet of the ACC, flows along the northern boundary of Drake Passage, measurements must resolve this strong flow up to the continental shelf—a challenge for satellite altimetry and gravity missions. Comprehensive reviews of ACC transport measurements in Drake Passage can be found in *Zlotnicki et al.* [2007], *Firing et al.* [2011], *Renault et al.* [2011], and *Meredith et al.* [2011].

In recent years, numerical and theoretical studies of the ACC have increasingly focused on along-path heterogeneity triggered by ACC-topographic interactions. For example, complex ridge and seamount structures have been shown to be hot spots of cross-frontal exchange [*Thompson and Sallée*, 2012] and regions where the partitioning of baroclinic and barotropic transport to the total transport changes over short distances [*Smith et al.*, 2010; *Peña-Molino et al.*, 2014; *Rintoul et al.*, 2014]. Here we use the term baroclinic (BC) transport to refer to transport constructed from geostrophic shears referenced to zero at the bottom and the term barotropic (BT) transport to denote the transport contribution from the bottom-reference velocity. These recent findings place strong demands upon the community to resolve the spatial and temporal structure of the ACC both numerically and observationally. The ACC's vertical and horizontal structure intimately links the mechanisms that transport mass, heat and other properties, both between oceanic basins and across the Southern Ocean, as well as where and how the ACC responds to atmospheric forcing [*Thompson and Naveira Garabato*, 2014].

Here we use a moored array that measured bottom currents across Drake Passage to determine the mean ACC BT transport. The cDrake experiment is introduced in section 2. The temporal stability of annual mean near-bottom current meters and their spatial structure across Drake Passage is presented in section 3. A mean BT transport estimate is given in section 4, and a concerted effort to determine its associated error bounds is provided in section 5. Section 6 combines our mean BT transport with the BC transport estimate from *Chidichimo et al.* [2014] and discusses the cDrake total transport estimate in the context of recent measurements.

2. cDrake Experiment

From November 2007 to November 2011, 19 CPIES and 3 short current meter moorings (termed the C line) were moored across Drake Passage (Figure 1) spanning from the tip of South America to the Antarctic Peninsula as part of the cDrake experiment [*Chereskin et al.*, 2009, 2012]. A CPIES is an inverted echo sounder and a pressure sensor housed together inside a glass sphere mounted on an anchor stand, with a current meter tethered 50 m overhead by additional flotation. Additional CPIES (termed the Local Dynamics Array, LDA) were placed midpassage northeast of the Shackleton Fracture Zone (SFZ) in a region of high eddy kinetic energy. To produce spatially coherent measurements, the CPIES were spaced approximately 30 to 60 km apart with shorter distances at the northern end of the line. Additionally, a tightly spaced array of five CPIES (termed the H-array) straddled the SFZ during the final year to resolve the deep flow bracketing the steep topographic feature (Figure 1 inset). Deployment years nominally span November to November.

The travel time measurements were used with hydrographic lookup tables to produce time series of geostrophic velocities referenced to zero at the bottom from which the mean BC transport and its variability were estimated [*Chidichimo et al.*, 2014]. Here we use the near-bottom currents to estimate the temporal mean depth-independent bottom-reference BT transport.

Details of the data return and processing are found in *Tracey et al.* [2013]. Here we focus on elements relevant to the near-bottom current records. The current meters were Aanderaa Doppler current sensors (DCS). Two model DCS heads were used: RCM-11 and Seaguard. The DCSs were mainly RCM-11s except during years 3 and 4 at sites C03 and C16 and year 4 at the H-array. Two corrections were applied: current directions were adjusted for the time-dependent local magnetic variation and current speeds were multiplied by a sound speed scale factor, the ratio of the local in situ sound speed to the constant value (1500 m s^{-1}) used during data acquisition. *Hogg and Frye* [2007] found that RCM-11s underestimated current speed when compared to vector-measuring current meters (VMCM) for speeds <20 cm s^{-1}, indicating that a speed correction might be needed. To address this concern, a four current-meter model intercomparison was conducted. Seven current meters consisting of four models (two VMCMs, two RCM-11s, two Seaguards, and a Nortek Aquadopp) were placed on a deep mooring in the LDA where we had observed strong deep currents (40–60 cm s^{-1}). Analysis of the 11 month records showed agreement within the expected current-meter accuracies of $\pm$0.15 cm s^{-1} [*Watts et al.*, 2013]. Thus, no current-meter model-dependent speed correction has been applied.

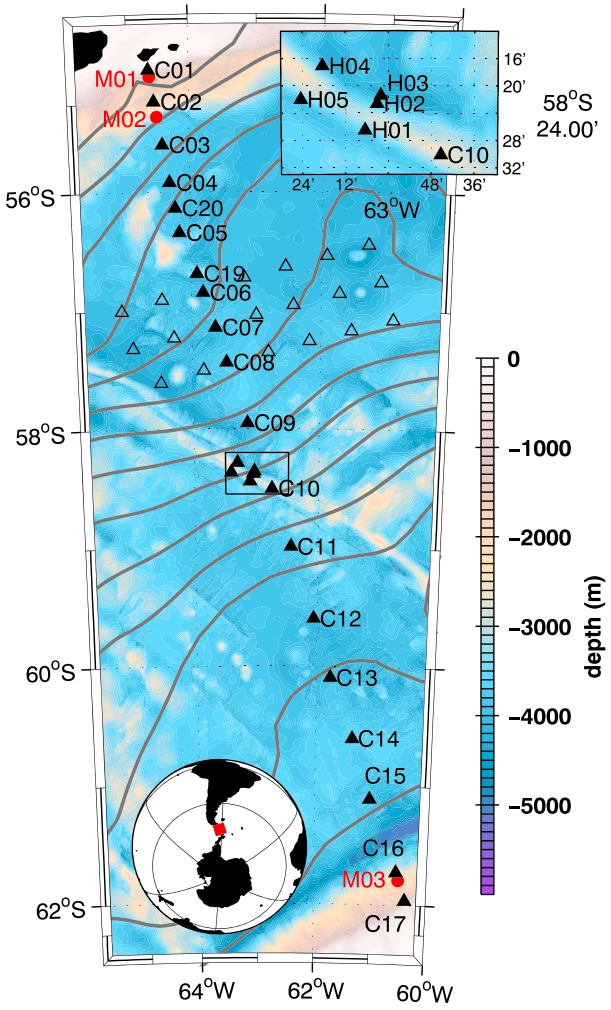

Figure 1. For 4 years, from November 2007 to November 2011, the cDrake moored array consisted of over 40 CPIES along a transport line (solid triangles) and in a local dynamics array (open triangles). During the first 2 years, three short current meter moorings were deployed at the continental margins (red circles). Additionally, five closely spaced CPIES (H01–H05) were deployed along the Shackleton Fracture Zone during the final year (black square and inset). The 4 year mean altimeter SSH (sea surface height above geoid also termed dynamic topography) is contoured with 10 cm intervals (gray lines). SSH is from the Ssalto/Duacs daily sea level anomaly products produced by the Copernicus Marine and Environment Monitoring Service and the mean dynamic topography (MDT) is the Centre National d'Etudes Spatiales (CNES) CLS13 produced by CLS Space Oceanography Division. Both altimeter products were distributed by Aviso with support from CNES (http://aviso.altimetry.fr/). Bathymetry is from *Ryan et al.* [2009], a product derived from shipboard multibeam measurements and *Smith and Sandwell* [1997].

Gaps in records occurred primarily due to leaks or cuts in current meter cables. Gaps occurred for the following years and instruments: year 1 has missing data for C04 and second half of year 1 for C01, year 2 has missing data for C02 and C03, year 3 has missing data for C08, and year 4 has missing data for C01. C05 returned a partial record during year 1 after which the CPIES was repositioned farther north. One year records exist at C12 (year 1) and the H-array (year 4). During the first 2 years, three short moorings equipped with Aanderaa RCM-8 current meters were deployed at the continental margins (red circles in Figure 1). On the northern slope, M01 returned records from current meters at 100, 300, and 600 m above the bottom; M02 returned only the 300 m above the bottom record. The southern slope mooring, M03, had two current meters at 100 and 300 m above the bottom. Velocity was typically measured once per hour. For instruments deployed in the final year with 10 min sampling, the measurements were averaged to hourly. All currents were low-pass filtered with a 3 day cutoff period and subsampled to twice daily.

3. Near-Bottom Currents

Topography and meandering ACC fronts influence the direction and strength of the mean near-bottom currents (Figure 2a). Strong mean currents, 5–13 cm s^{-1}, flow along steep topography associated with the SFZ and the continental slopes. Note in Figure 2a, the H01, H02, and H03 sites have been translated southeastward along topography so that they fall on the C line while maintaining the same deployment depth. In general, mean near-bottom currents are not aligned with mean SSH contours except along the northern boundary where both the SAF and near-bottom currents flow parallel to the continental slope. Strong near-bottom flow also exists in the central passage: for example, at C08 and C09 mean speeds are near 10 cm s^{-1}. Here in the LDA, deep cyclogenesis occurs repeatedly when ACC meanders develop in concert with deep eddy formation [*Chereskin et al.*, 2009]. In the eastern portion of the LDA within the Yaghan Basin, a deep cyclonic circulation exists. South of 60°S the mean currents in the deep passage are weaker, typically less than 6 cm s^{-1}. Eastward flow at C12 and northwestward flow at C13 suggest a possible localized circulation associated with a topographic depression. Figure 2a indicates that along the C line a bottom reference velocity of zero is not appropriate and that high-horizontal resolution is required to determine the mean BT transport.

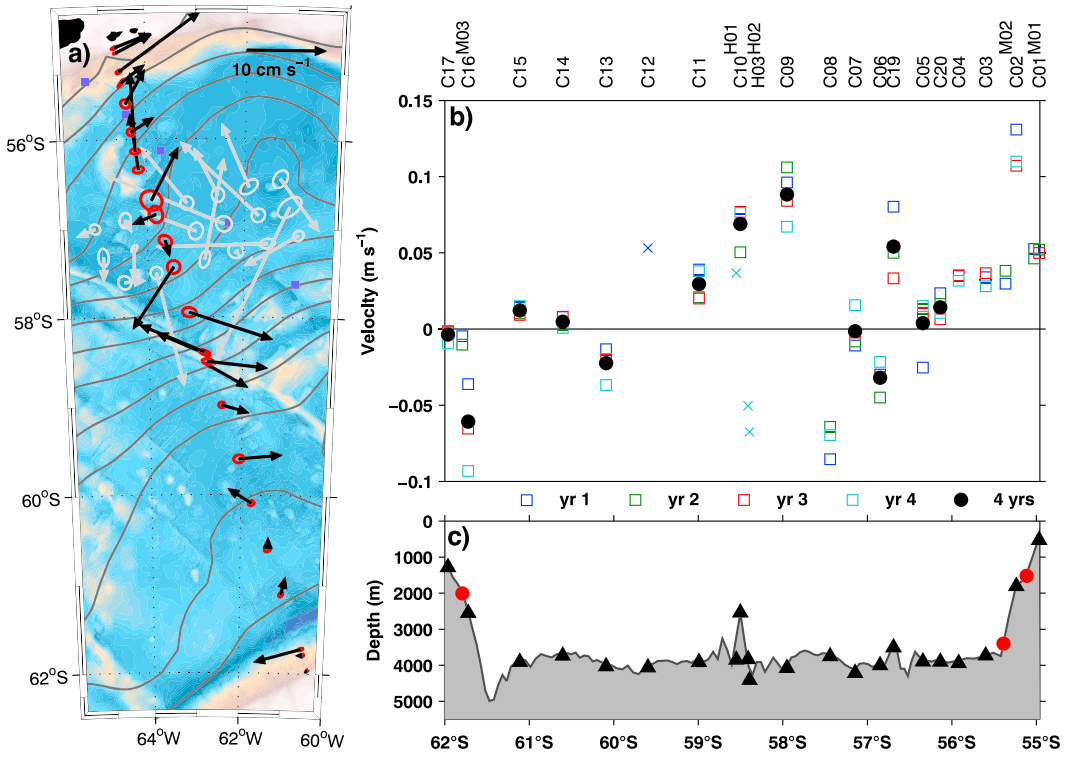

Figure 2. (a) Record-length mean near-bottom currents and standard error ellipses (C line denoted by black arrows and LDA denoted by gray arrows). Blue squares mark the locations of the *Koenig et al.* [2014] Yaghan Basin moorings. (b) Annual means (open squares) and 4 year averages (black circles) for near-bottom currents perpendicular to the transport line, u_T. One year records at C12, H01, H02, and H03 are indicated by crosses. (c) Bottom topography along the transport line with CPIES (triangles) and current meter mooring (circles) locations indicated.

Means are remarkably stable. Standard error ellipses are small compared to the record-length mean currents (Figure 2a). Standard errors of the mean are small and range from 0.2 to 1.1 cm s^{-1}, with average radius of 0.7 cm s^{-1}. Table S1 in the supporting information provides the record mean near-bottom currents at the C line sites. Measured currents were rotated into a coordinate system oriented along and across the instrumented line, and the component perpendicular to the line, termed u_T, was used to calculate BT transport. Along-passage means are robust as indicated by the strikingly uniform mean u_T for individual years. Figure 2b illustrates how similar the 1 year means are for multiple-year sites. Using two-sample *t* tests, we determined that for 19 out of the 21 multiple-year sites, no 1 year mean was statistically different from another nor statistically different from the site record-length mean at the 95% confidence level. Note that the standard error ellipses and standard error of the mean calculations require an estimate of the degrees of freedom. Following the methodology from *Bendat and Piersol* [2000, p. 173], degrees of freedom are calculated from the measurements' autocorrelations. Typically, every ~10 days provides a degree of freedom. Figure 2b and our statistical tests provide confidence that available cDrake deep current-meter measurements with record lengths of at least 1 year can be used to resolve the structure of the BT current across the C line.

4. Mean Barotropic Transport

The mean through-passage BT transport is 45.6 Sv with an uncertainty of 8.9 Sv (Figure 3). BT volume transport is calculated using trapezoidal integration of the near-bottom mean current multiplied by the site-dependent water depth. For a few sites near steep topography, the integration was distance weighted to account for variations in spatial correlation length scales. Details about these weightings and errors are discussed in the next section. If the flow were distributed uniformly across the passage, this mean transport would correspond to a mean through-passage bottom-reference velocity of 1.3 cm s^{-1}.

South of 60°S, the mean BT transport is weak and slightly westward. Little transport accumulates across the SFZ due to the counterflows on either side of the ridge. Through-passage transport accumulates northward

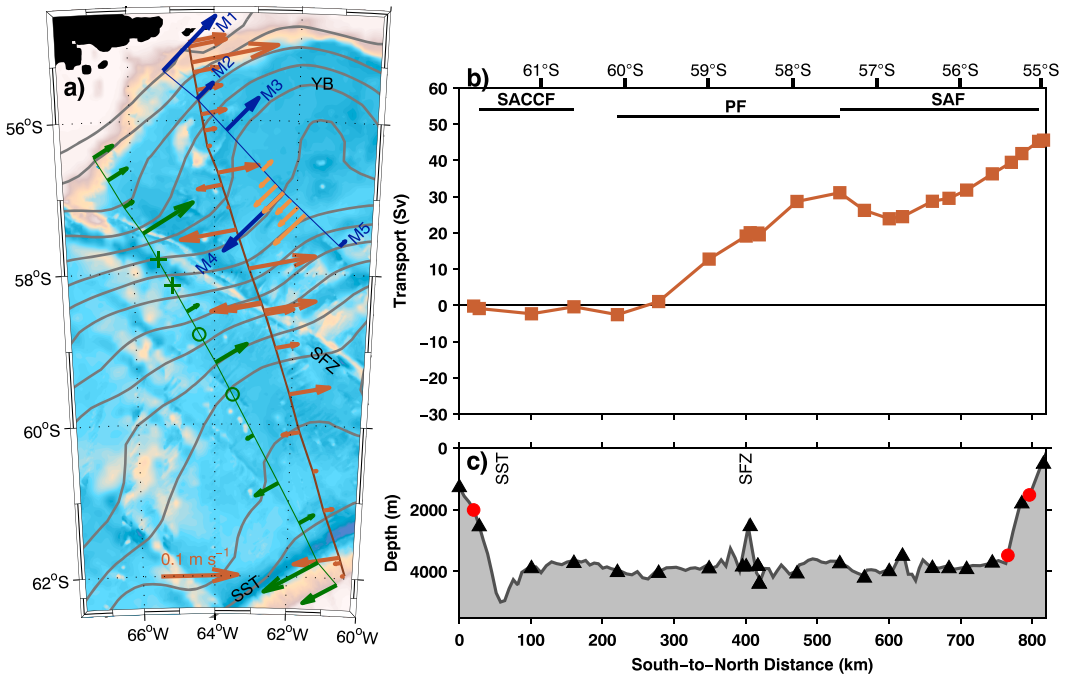

Figure 3. (a) Record-length mean near-bottom currents perpendicular to the transport line (brown vectors) used to determine the mean barotropic transport. Near-bottom currents perpendicular to Jason track 104 from Figure 14 of *Koenig et al.* [2014] (blue vectors) and cDrake (orange vectors). ISOS 2500 m depth currents rotated perpendicular to the ISOS line shown with green vectors. For the ISOS line, pluses indicate lost moorings; open circles indicate lost deep current meters. Topographic features, the South Shetland Trench (SST), Yaghan Basin (YB), and Shackleton Fracture Zone (SFZ) are labeled. (b) Cumulative through-passage barotropic transport integrated from south to north (brown line). Horizontal bars indicate the nominal ranges of the Subantarctic Front (SAF), Polar Front (PF), and Southern ACC Front (SACCF). (c) Bottom topography with CPIES (triangles) and current meter mooring (circles) locations indicated. Two prominent topographic features are noted: SFZ near 58.5°S and SST near 61.5°S.

across the passage beneath the PF and SAF. The slight transport decrease near 600 km (56.8°S) is associated with the deep mean anticyclonic and cyclonic flows in the Yaghan Basin (Figure 3). The 45.6 Sv of through-passage BT transport is nearly evenly partitioned between the PF and SAF; integrating from 278 to 600 km (59.60°S to 56.8°S), the deep mean PF contributes 23 Sv. This broad extent, 322 km, is due to the variability in the position of the PF. Using the cDrake data set, *Foppert et al.* [2016] showed that the PF along the C line has bimodal structure: existing north and south of the SFZ at separate times. In the *Foppert et al.* [2016] stream-coordinate analysis, the barotropic transport of PF, regardless of its location, is equal to about 20 Sv, consistent with this Eulerian analysis.

5. Error Sources

We consider the following six error sources for the BT transport estimate: instrument uncertainty, temporal sampling uncertainty, spatial sampling uncertainty for the array as a whole as well as near the southern slope and near the SFZ, and finally, possible near-bottom intensification. Propagation of the site-to-site-independent instrument error of 0.15 cm s^{-1} through the transport calculation yielded an error of 1.1 Sv. To address the temporal sampling uncertainty, the standard error of the mean for each site was propagated through the transport calculation to yield a 5.5 Sv error.

Our overarching assumption is that the measured mean currents resolved the mean transport both within the closely resolved continental slope and SFZ regions, and within the broad channel. Supporting evidence comes from the transverse velocity correlations, 8 of 12 neighboring site pairs in the broad channel were significant at the 95% confidence level. The array-wide uncertainty arises from the spatial resolution of the CPIES locations. Using objective analysis, we produced formal estimates of the barotropic geostrophic stream function error. *Firing et al.* [2014] describe methods to determine the barotropic geostrophic streamfunction, ψ, with objective analysis using current, pressure, or geopotential height anomaly and also discuss methods

to determine dimensional error estimates. We apply their methodology to determine the accumulated ψ error using only currents as inputs. The correlation function for pressure is given by a Gaussian, $\exp(-\lambda\gamma^2)$, where $\lambda = 1/L^2$, where L is the correlation length scale determined from the bottom pressure records and γ is the separation distance between measurements. Corresponding longitudinal and transverse correlation functions are $\exp(-\lambda\gamma^2)$ and $(1 - 2\lambda\gamma^2)\exp(-\lambda\gamma^2)$, respectively. The objective analysis yields a percent error variance estimate that depends on γ, L, and noise-to-signal ratios, E. As in *Firing et al.* [2014], the dimensional error is recovered by multiplying the percent error variance by the measurement variance. The transport error is $D\sqrt{e_{\psi_{\text{north}}} + e_{\psi_{\text{south}}}}$, where D is the mean depth and $e_{\psi_{\text{north}}}$ and $e_{\psi_{\text{south}}}$ are the dimensional error variances for the northernmost and southernmost ψ, respectively. To explore the sensitivity of the transport error estimate, we considered 60, 90, 120, 180, and 240 day low-passed filtered currents as inputs to the objective analysis. For each low-pass test, we implemented a suite of correlation lengths (60, 75, 120,and 200 km) and E values (0.1, 0.15, and 0.20). The ensemble mean error decreases as the low-pass filter length increases: 7.3 Sv for the 60 day, 6.4 Sv for the 90 day, 5.7 Sv for the 120 day, 4.9 Sv for the 180 day, and 4.6 Sv for the 240 day low-pass tests. Because the longer low-passed filtered currents resemble the mean flow ever more closely, we argue that the 240 day low-pass estimate of 4.6 Sv represents the mean transport error associated with spatial sampling uncertainty for the array as a whole.

An additional spatial sampling error pertains to sites near steep topography where correlation scales decrease. To account for this, the contribution from each site was weighted by a distance from the nearby bathymetric feature. Distance-weighted trapezoidal integration was used at the southern continental slope and at the SFZ. (see the supporting information Figure S1). At the southern end, we assumed that C16's influence extended 24 km from the slope. Varying this distance between 24 and 36 km gave rise to an error of 1.8 Sv at the southern slope. For H01 and H03, we considered this distance to be 15 km from the SFZ. Varying this distance between 10, 15, and 20 km gave rise to uncertainty estimate 2.8 Sv for the SFZ region.

Finally, in our application we assume that the currents measured at 50 m above the bottom are outside the bottom boundary layer and depth independent. Because this is a region of sloping topography, it is possible that some bottom intensification occurs as was found in the Kuroshio Extension [*Bishop et al.*, 2012]. If, instead, we assume a hyperbolic decay such that the speeds at the surface are 80% of those at depth, we estimate a bottom-trapping bias error of 4 Sv. Summing the error variance contributions together, an uncertainty of $\sqrt{1.1^2 + 5.5^2 + 4.6^2 + 2.8^2 + 1.8^2 + 4^2} = 8.9$ Sv is obtained for the mean BT transport.

6. Discussion and Conclusion

Combining the cDrake BC transport of 127.7 ± 5.9 Sv from *Chidichimo et al.* [2014] with the BT transport of 45.6 ± 8.9 Sv yields 173.3 ± 10.7 Sv. This cDrake total transport is 30% higher than the canonical value of 134 Sv from the ISOS experiment [*Whitworth et al.*, 1982; *Whitworth*, 1983; *Whitworth and Peterson*, 1985]. *Cunningham et al.*'s [2003] revised ISOS error estimate of 27 Sv gives a maximum transport of 161 Sv, which nearly reaches the cDrake minimum estimate of 163 Sv. The ISOS mean transport estimate relied on referencing three hydrographic surveys with the current meter moorings. ISOS mean near-bottom currents rotated perpendicular to their line are shown in Figure 3 by green vectors. Two critical moorings were lost in northern Drake Passage between the SAF and PF resulting in a ~87 km gap. There is no good way to fill those gaps by an attempted projection of currents from the cDrake back to the ISOS line, because deep currents do not follow the same path as the upper currents; instead, they are steered by mountain ranges and flow around deep recirculations. Nevertheless, we can simulate the effect of losses by omitting from cDrake sites C08, C09, or both sites such that they leave comparable midpassage gaps of 35, 60, and 95 km, respectively; resulting BT transports determined by trapezoidal integration across the gaps are 65, 3, and 34 Sv. This highlights the sensitivity of the total transport calculation to loss of moorings in the strong deep currents between the SAF and PF. In cDrake, bottom currents were measured across Drake Passage with unprecedented spatial and temporal resolution and duration. Horizontal resolution was comparable to ISOS south of the PF and along the continental boundaries, however, midpassage where these ACC jets reside and significant BT transport accrues, cDrake more than doubled the number of measurements. *Meredith and Hughes* [2005] stress the requirement for higher than weekly averaging to resolve the mean ACC transport due to rapid transport fluctuations. cDrake resolved these fluctuations by measuring bottom currents hourly, and at most sites for 4 years, whereas the ISOS mean estimate derived mainly from three referenced hydrographic sections conducted at the beginning, middle, and end of the 1 year deployment.

Three recent estimates of total transport through Drake Passage exist. These estimates are independent of one another as they rely on different data sets. Using high-horizontal resolution directly measured SADCP velocity data taken between 2004 and 2009 across Drake Passage, *Firing et al.* [2011] estimated the mean total transport in the upper 1000 m to be 95 ±2 Sv. For cDrake, we calculated the BC and BT contributions in the upper 1000 m to be 77 ± 4 Sv and 13 ± 2 Sv, respectively. These combine to give a total of 90 ± 5 Sv, which is in agreement with the estimate from direct velocity measurements. Recently, through a combination of current meter moorings and altimetry, *Koenig et al.* [2014] determined a mean Drake Passage transport of 141 Sv. Our total transport estimates are higher, mainly due to the strong cDrake BT contribution of 45.6 Sv compared to their 5 Sv. They used empirical lookups between the surface velocity and the depth-dependent velocity structure from moored current meters spaced 65 to 120 km apart along Jason track 104 (Figure 2) and extrapolated velocity from their deepest measurements (e.g., 3000 m and 2500 m depth at their M3 and M4, respectively) to the seafloor. In the *Koenig et al.* [2014] construction, extrapolated estimates of bottom speed (Figure 3, blue vectors) are nearly twice that from a colocated cDrake site (Figure 3, orange vectors). Moreover, their lateral extent of the Yaghan Basin deep cyclonic recirculation appears artificially broad with deep cross-transect speeds changing from negative to positive near 56.5°S (their Figure 14), while cDrake contemporaneous observations resolve this circulation to be much narrower. Their study had only one mooring in the deep recirculation gyre; the effect of the mooring spacing is to broaden this recirculation and overemphasize its westward transport contribution. We surmise that a combination of inadequate spatial resolution in the *Koenig et al.* [2014] observations and along-path variability contribute to the discrepancies between the two estimates. Finally, *Colin de Verdière and Ollitrault* [2016] combined Argo float displacements and historical hydrography from the World Ocean Atlas 2009 to determine a global mass conserving mean circulation. They found 175 Sv transport through Drake Passage. In summary, our cDrake estimate is in agreement with two of the three other recent estimates.

We attribute the 30% increase relative to the ISOS estimate to improvements in the measurement systems. Absolute transports are difficult to measure in the ocean. Basin-wide transport calculations are often constrained by zero or near-zero mass-flux conditions, a requirement that cannot be applied to the ACC. The approach by *Colin de Verdière and Ollitrault* [2016] circumvents this issue due to its global approach. While the cDrake annual mean near-bottom velocities are remarkably stable, the deep circulation shows a complex pattern and highlights the requirement for spatially well-resolved measurements, such as cDrake and the *Firing et al.* [2011] SADCP study, for the transport estimate. Analysis of the Southern Ocean State Estimate by *Peña-Molino et al.* [2014] shows that the relative contribution of BT/BC transports to total ACC transport varies along its path. In regions of complex topography, the mean BT contribution can be as high as 50%. Along the C line, the BT transport contributes 27% to the mean total transport. Based upon *Peña-Molino et al.* [2014], our BT/BC partitioning should be considered regionally specific to the cDrake location.

We do not ascribe the 30% increase as due to the ocean's response to the increasing strength of Southern Ocean winds over the past few decades. This conclusion is supported by recent analysis of satellite altimetry and numerical simulations. *Hogg et al.* [2015] examined the altimeter record and found that Southern Ocean eddy kinetic energy has increased over the 20+ year altimeter record, yet using sea level along the southern boundary as a proxy for ACC transport, ACC transport has remained relatively steady, exhibiting a slight decrease. They found that decadal trends in increased wind stress, increased eddy kinetic energy, and steady transport were supported by their eddy-resolving numerical simulations. Analysis of a 0.1° ocean, 0.25° atmosphere, global climate simulation forced by winds that were increased by 50% south of 30° S shows that Drake Passage transport increased only 6% compared to control runs [*Bishop et al.*, 2016]. A 6% increase in transport would be similar to the difference between *Cunningham et al.* [2003]'s ISOS upper bound of 161 Sv and cDrake's 173.3 Sv.

Acknowledgments
We thank the captains and crew of the RVIB Nathaniel B. Palmer and the Antarctic Support Contractor, Raytheon Polar Services, for their support of the cDrake field operations. NSF Office of Polar Programs supported this work under grants to URI (ANT-0635437; ANT-1141802) and UCSD (ANT-0636493; ANT-1141922). The data are available through NOAA National Centers for Environmental Information, Accession0121256.

References

Bendat, J., and A. Piersol (2000), *Random Data: Analysis and Measurement Procedures*, 3rd ed., Wiley, New York.

Bishop, S. P., D. R. Watts, J.-H. Park, and N. G. Hogg (2012), Evidence of bottom-trapped currents in the Kuroshio Extension region, *J. Phys. Oceanogr.*, *42*(2), 321–328, doi:10.1175/JPO-D-11-0144.1.

Bishop, S. P., P. R. Gent, F. O. Bryan, A. F. Thompson, M. C. Long, and R. Abernathey (2016), Southern Ocean overturning compensation in an eddy-resolving climate simulation, *J. Phys. Oceanogr.*, *46*(5), 1575–1592, doi:10.1175/JPO-D-15-0177.1.

Bryden, H. L., and R. D. Pillsbury (1977), Variability of deep flow in the Drake Passage from year-long current measurements, *J. Phys. Oceanogr.*, *7*(6), 803–810.

Chereskin, T. K., K. A. Donohue, D. R. Watts, K. L. Tracey, Y. Firing, and A. L. Cutting (2009), Strong bottom currents and cyclogenesis in Drake Passage, *Geophys. Res. Lett.*, *36*, L23602, doi:10.1029/2009GL040940.

Chereskin, T. K., K. A. Donohue, and D. R. Watts (2012), cDrake: Dynamics and transport of the Antarctic Circumpolar Current in Drake Passage, *Oceanography*, *25*(3), 134–135.
Chidichimo, M. P., K. A. Donohue, D. R. Watts, and K. L. Tracey (2014), Baroclinic transport time series of the Antarctic Circumpolar Current measured in Drake Passage, *J. Phys. Oceanogr.*, *44*(7), 1829–1853, doi:10.1175/JPO-D-13-071.1.
Colin de Verdière, A., and M. Ollitrault (2016), A direct determination of the World Ocean barotropic circulation, *J. Phys. Oceanogr.*, *46*(1), 255–273, doi:10.1175/JPO-D-15-0046.1.
Cunningham, S., S. Alderson, B. King, and M. Brandon (2003), Transport and variability of the Antarctic Circumpolar Current in Drake Passage, *J. Geophys. Res.*, *108*(C5), 8084, doi:10.1029/2001JC001147.
Firing, Y., T. K. Chereskin, and M. R. Mazloff (2011), Vertical structure and transport of the Antarctic Circumpolar Current in Drake Passage from direct velocity measurements, *J. Geophys. Res.*, *116*, C08015, doi:10.1029/2011JC006999.
Firing, Y. L., T. K. Chereskin, D. R. Watts, K. L. Tracey, and C. Provost (2014), Computation of geostrophic streamfunction, its derivatives, and error estimates from an array of CPIES in Drake Passage, *J. Atmos. Ocean. Tech.*, *31*(3), 656–680, doi:10.1175/JTECH-D-13-00142.1.
Foppert, A., K. A. Donohue, and D. R. Watts (2016), The Polar Front in Drake Passage: A composite-mean stream-coordinate view, *J. Geophys. Res. Oceans*, *121*, 1771–1788, doi:10.1002/2015JC011333.
Hogg, A. M., M. P. Meredith, D. P. Chambers, E. P. Abrahamsen, C. W. Hughes, and A. K. Morrison (2015), Recent trends in the Southern Ocean eddy field, *J. Geophys. Res. Oceans*, *120*, 257–267, doi:10.1002/2014JC010470.
Hogg, N. G., and D. E. Frye (2007), Performance of a new generation of acoustic current meters, *J. Phys. Oceanogr.*, *37*(2), 148–161, doi:10.1175/JPO3003.1.
Koenig, Z., C. Provost, R. Ferrari, N. Sennéchael, and M.-H. Rio (2014), Volume transport of the Antarctic Circumpolar Current: Production and validation of a 20 year long time series obtained from in situ and satellite observations, *J. Geophys. Res. Oceans*, *119*, 5407–5433, doi:10.1002/2014JC009966.
Meredith, M. P., and C. W. Hughes (2005), On the sampling timescale required to reliably monitor interannual variability in the Antarctic circumpolar transport, *Geophys. Res. Lett.*, *32*, L03609, doi:10.1029/2004GL022086.
Meredith, M. P., et al. (2011), Sustained monitoring of the Southern Ocean at Drake Passage: Past achievements and future priorities, *Rev. Geophys.*, *49*, RG4005, doi:10.1029/2010RG000348.
Peña-Molino, B., S. R. Rintoul, and M. R. Mazloff (2014), Barotropic and baroclinic contributions to along- and across-stream transport in the Antarctic Circumpolar Current, *J. Geophys. Res. Oceans*, *119*, 8011–8028, doi:10.1002/2014JC010020.
Renault, A., C. Provost, N. Sennéchael, N. Barré, and A. Kartavsteff (2011), Two full-depth velocity sections in the Drake Passage in 2006—Transport estimates, *Deep Sea Res., II*, *58*(25), 2572–2591.
Rintoul, S. R., S. Sokolov, M. J. M. Williams, B. Peña-Molino, M. Rosenberg, and N. L. Bindoff (2014), Antarctic Circumpolar Current transport and barotropic transition at Macquarie Ridge, *Geophys. Res. Lett.*, *41*, 7254–7261, doi:10.1002/2014GL061880.
Ryan, W. B. F., et al. (2009), Global multi-resolution topography synthesis, *Geochem. Geophys. Geosyst.*, *10*, Q03014, doi:10.1029/2008GC002332.
Smith, I. J., D. P. Stevens, K. J. Heywood, and M. P. Meredith (2010), The flow of the Antarctic Circumpolar Current over the North Scotia Ridge, *Deep Sea Res.*, *57*(1), 14–28, doi:10.1016/j.dsr.2009.10.010.
Smith, W. H., and D. T. Sandwell (1997), Global sea floor topography from satellite altimetry and ship depth soundings, *Science*, *277*, 1956–1962, doi:10.1126/science.277.5334.1956.
Thompson, A., and A. Naveira Garabato (2014), Equilibration of the Antarctic Circumpolar Current by standing meanders, *J. Phys. Oceanogr.*, *44*, 1811–1828, doi:10.1175/JPO-D-13-0163.1.
Thompson, A. F., and J.-B. Sallée (2012), Jets and topography: Jet transitions and the impact on transport in the Antarctic Circumpolar Current, *J. Phys. Oceanogr.*, *42*, 956–972, doi:10.1175/JPO-D-11-0135.1.
Tracey, K. L., K. A. Donohue, D. R. Watts, and T. Chereskin (2013), cDrake CPIES data report, *GSO Tech. Rep. 2013-01*, Graduate School of Oceanography, Univ. of Rhode Island.
Watts, D. R., M. A. Kennelly, K. A. Donohue, K. L. Tracey, T. K. Chereskin, R. A. Weller, and I. Victoria (2013), Four current meter models compared in strong currents in Drake Passage, *J. Atmos. Oceanic Technol.*, *30*(10), 2465–2477, doi:10.1175/JTECH-D-13-00032.1.
Whitworth, T. (1983), Monitoring the transport of the Antarctic Circumpolar Current at Drake Passage, *J. Phys. Oceanogr.*, *13*(11), 2045–2057.
Whitworth, T., and R. Peterson (1985), Volume transport of the Antarctic Circumpolar Current from bottom pressure measurements, *J. Phys. Oceanogr.*, *15*(6), 810–816.
Whitworth, T., W. Nowlin, and S. Worley (1982), The net transport of the Antarctic Circumpolar Current through Drake Passage, *J. Phys. Oceanogr.*, *12*(9), 960–971.
Zlotnicki, V., J. Wahr, I. Fukumori, and Y. T. Song (2007), Antarctic Circumpolar Current transport variability during 2003–05 from GRACE, *J. Phys. Oceanogr.*, *37*(2), 230–244, doi:10.1175/JPO3009.1.